

# VU Research Portal

## **Predissociation in b1Pu, v (v=1,4,5,6) levels of N2**

Ubachs, W.M.G.; Velchev, I.; de Lange, A.

### ***published in***

Journal of Chemical Physics  
2000

### ***DOI (link to publisher)***

[10.1063/1.481145](https://doi.org/10.1063/1.481145)

### ***document version***

Publisher's PDF, also known as Version of record

[Link to publication in VU Research Portal](#)

### ***citation for published version (APA)***

Ubachs, W. M. G., Velchev, I., & de Lange, A. (2000). Predissociation in b1Pu, v (v=1,4,5,6) levels of N2. *Journal of Chemical Physics*, 112, 5711-5615. <https://doi.org/10.1063/1.481145>

### **General rights**

Copyright and moral rights for the publications made accessible in the public portal are retained by the authors and/or other copyright owners and it is a condition of accessing publications that users recognise and abide by the legal requirements associated with these rights.

- Users may download and print one copy of any publication from the public portal for the purpose of private study or research.
- You may not further distribute the material or use it for any profit-making activity or commercial gain
- You may freely distribute the URL identifying the publication in the public portal ?

### **Take down policy**

If you believe that this document breaches copyright please contact us providing details, and we will remove access to the work immediately and investigate your claim.

### **E-mail address:**

[vuresearchportal.ub@vu.nl](mailto:vuresearchportal.ub@vu.nl)

# Predissociation in $b^1\Pi_u, v(v=1,4,5,6)$ levels of $N_2$

W. Ubachs,<sup>a)</sup> I. Velchev, and A. de Lange

Department of Physics and Astronomy, Vrije Universiteit, De Boelelaan 1081,  
1081 HV Amsterdam, The Netherlands

(Received 4 November 1999; accepted 11 January 2000)

In a high-resolution laser spectroscopic study, using a tunable Fourier-transform limited light source in the extreme ultraviolet, the  $b^1\Pi_u$  excited valence state of molecular nitrogen is reinvestigated for vibrational levels  $v=1, 4, 5$ , and  $6$ . From line broadening of individual rotational levels excited state lifetimes were determined:  $\tau_{(v=1)}=1.1\pm0.3$  ns,  $\tau_{(v=4)}=18\pm1$  ps,  $\tau_{(v=5)}=205\pm25$  ps, and  $\tau_{(v=6)}=350\pm75$  ps. Additionally, the lifetime of the  $o_3^1\Pi_u, v=0$  Rydberg state was determined:  $\tau=240\pm50$  ps. For the  $b^1\Pi_u, v=1$  state improved rotational constants were determined. © 2000 American Institute of Physics. [S0021-9606(00)02113-9]

## I. INTRODUCTION

Dissociation of molecular nitrogen is an important process initiating chemical reactions in the upper layers of the Earth's atmosphere.<sup>1</sup> All excited singlet states to which a dipole-allowed transition is possible from the electronic ground state lie above both the  $N(^4S)+N(^4S)$  and  $N(^4S)+N(^2D)$  dissociation limits.<sup>2</sup> One of the mechanisms leading to dissociation is predissociation via excited states of *ungerade* symmetry upon electron impact; this process occurs in the aurorae.<sup>3</sup> Most of the excited states of *u* symmetry in the energy range 100 000–115 000  $\text{cm}^{-1}$  undergo strong dissociation, with the notable exception of the  $c_4^1\Sigma_u^+, v=0$  Rydberg state and the  $b^1\Pi_u, v=1$  valence state, which are known to produce intense extreme ultraviolet (XUV) and near UV emissions. From detailed studies<sup>4</sup> it has been deduced that the  $b^1\Pi_u$  state contributes for 6% to the dissociation budget for electron impact at 100 eV. After previous work on the states of  $^1\Sigma_u^+$  symmetry in our group<sup>5</sup> the focus of the present investigation is on the  $b^1\Pi_u$  state, which is the upper state of the Birge–Hopfield system.<sup>6</sup> The  $b^1\Pi_u-X^1\Sigma_g^+$  band system was investigated by Carroll and Collins<sup>7</sup> in, by the standard of classical spectroscopy, high resolution absorption. The peculiar intensity distribution over vibrational bands, strongly deviating from expectations based on Franck–Condon factors, was later explained by Stahel, Leoni, and Dressler.<sup>8</sup> Homogeneous coupling between the  $b^1\Pi_u$  valence state with the lowest Rydberg state  $c_3^1\Pi_u$ , and the lowest Rydberg state  $o_3^1\Pi_u$  converging to the electronically excited  $N_2^+$  ion ( $A^2\Pi_u$ ), give rise to destructive interference, thereby lowering the intensity at  $b^1\Pi_u, v=5$  and  $6$ .

A second irregular feature in  $b^1\Pi_u$  is the variation of the predissociation rate as a function of vibrational quantum number. This issue was addressed by Leoni and Dressler,<sup>9</sup> who found a high predissociation rate for  $b^1\Pi_u, v=3$ . Later quantitative predissociation rates for  $b^1\Pi_u, v=0-5$  were determined by Ubachs, Tashiro, and Zare.<sup>10</sup> The mechanism for this subtle predissociation behavior has been discussed in

the literature;<sup>4,9,10</sup> it is attributed to interaction with  $C'^3\Pi_u$ ,  $C^3\Pi_u$ , and  $F^3\Pi_u$  states but not yet fully explained. In a study using synchrotron excitation strong vacuum-ultraviolet fluorescence was observed from  $b^1\Pi_u, v=1$ .<sup>11</sup> This was verified in an extensive study by James *et al.*,<sup>4</sup> who estimated that 95% of electron-impact induced emission from the  $b^1\Pi_u$  state originates from the  $v=1$  level. They further estimated that all  $b^1\Pi_u$  vibrational levels predissociate with a yield of virtually 100%, except for three levels with predissociation fractions of 10% ( $v=1$ ), 96% ( $v=6$ ), and 98% ( $v=7$ ). In a recent high-resolution spectroscopic study by Roncin and Launay, emission was observed in the  $b^1\Pi_u-X^1\Sigma_g^+(v',v'')$  bands for  $v'=1, 6$ , and  $7$ , but also for  $v'=5$ .<sup>12</sup> In the latter work emission bands originating in  $c_3^1\Pi_u, v=1-2$  and  $o_3^1\Pi_u, v=0-3$  states of Rydberg character were observed, indicating that predissociation from these levels is also less than 100%.

In this work several  $b^1\Pi_u$  vibrational levels are reinvestigated using a highly coherent tunable laser source in the extreme ultraviolet. From line broadening measurements upper state lifetimes and predissociation rates are determined in a molecular beam experiment. Transition frequencies for several rotational lines in the  $b^1\Pi_u-X^1\Sigma_g^+(1,0)$  band are determined at very high accuracy, yielding improved rotational constants for the  $b^1\Pi_u, v=1$  state.

## II. EXPERIMENT

The experimental setup is similar to the one used previously for the study of the  $1SU^+$  so ungerade states of  $N_2$ ,<sup>5</sup> while details of the experimental methods are explained in Ref. 13. Tunable XUV radiation is produced with a laser system consisting of a chain of a stabilized cw-ring dye laser in the range 570–600 nm, a pulsed-dye-amplifier pumped by a powerful Nd-YAG laser, frequency-doubling in a KDP crystal, and third-harmonic generation in a pulsed jet of xenon gas. This chain delivers coherent XUV light with a bandwidth in the range 250–350 MHz, dependent on specific conditions in the dye amplifier. The procedure to determine linewidths of the  $N_2$  resonances, including the deconvolution of the instrument width, is similar to the one used in our

<sup>a)</sup>Electronic mail: wimu@nat.vu.nl

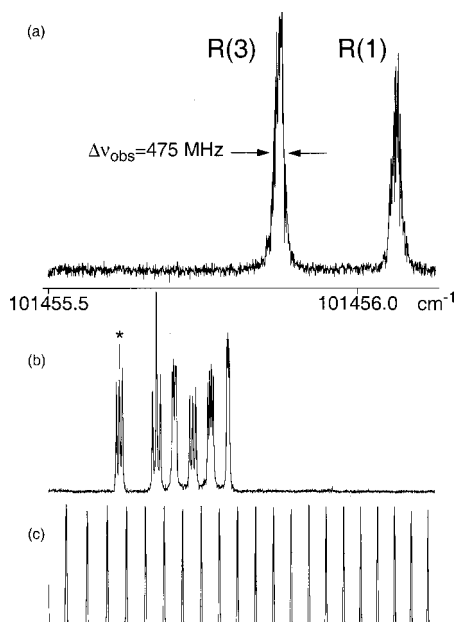


FIG. 1. (a) Spectrum of the  $R(1)$  and  $R(3)$  lines in the  $b^1\Pi_u-X^1\Sigma_g^+(1,0)$  band of  $N_2$  at  $\lambda=98.56$  nm recorded with the pulsed tunable XUV source; (b) simultaneously recorded  $I_2$  saturation spectrum for absolute calibration with the cw output of the ring dye laser at the fundamental wavelength  $\lambda=591.39$  nm; the line marked with an asterisk is the “ $t$ ” hyperfine component of the  $B-X(13-1)$   $R95$  line of  $I_2$  at  $16\,909.266\,00\text{ cm}^{-1}$ ; (c) simultaneously recorded etalon markers with  $\text{FSR}=148.9560\text{ MHz}$ .

previous studies.<sup>13</sup> The value for the instrument width involves for the most part the bandwidth of the XUV source and an additional effect of residual Doppler broadening in the crossed beam configuration. The latter depends on the specific geometry chosen, the diameters of the nozzle opening and skimmer, as well as the divergence of the XUV beam.

Spectroscopy of  $N_2$  is performed via 1 XUV+1 UV photoionization in a setup where the XUV beam is perpendicularly crossed with a collimated beam of pure nitrogen gas obtained from a pulsed valve. In the collision-free expanding jet of  $N_2$  only the lowest rotational states were accessible for investigation. Simultaneously with the  $N_2$  spectra in the XUV domain the visible output from the cw-ring dye laser was used to record markers of a stabilized etalon [free spectral range  $148.9560$  (5) MHz] and a saturated absorption spectrum of molecular iodine for absolute frequency calibration. The accurately calibrated reference lines were obtained either from Ref. 14 or specifically calibrated in our laboratory during the measurements.

### III. RESULTS

#### A. Spectroscopy of $b^1\Pi_u$ , $v=1$

In Fig. 1 a spectral recording of the  $R(1)$  and  $R(3)$  lines of the  $b^1\Pi_u-X^1\Sigma_g^+(1,0)$  band is shown with simultaneously recorded etalon and  $I_2$  reference spectra. The superior characteristics of the tunable XUV source allow one for the first time to fully resolve these lines in this bandhead region. The line marked with asterisk in the  $I_2$  reference spectrum is the “ $t$ ” hyperfine component of the  $R95$  transition in the  $B-X(13-1)$  band of  $I_2$  at  $16\,909.266\,00$  (7)

TABLE I. Accurately calibrated lines in the  $b^1\Pi_u-X^1\Sigma_g^+(1,0)$  band of  $N_2$  and deviations from a least-squares fit. Note that in the listed frequencies a possible systematic overall shift of  $\pm 0.003\text{ cm}^{-1}$ , due to the chirp effect, is not accounted for.

Line	Frequency ( $\text{cm}^{-1}$ )	Obs.-calc.
$R(0)$	$101\,454.411 \pm 0.001$	0.001
$R(1)$	$101\,456.062 \pm 0.001$	-0.001
$R(2)$	$101\,456.551 \pm 0.001$	0.000
$R(3)$	$101\,455.873 \pm 0.001$	-0.002
$R(4)$	$101\,454.031 \pm 0.001$	-0.001
$Q(2)$	$101\,448.105 \pm 0.001$	0.000
$Q(3)$	$101\,444.615 \pm 0.001$	0.000
$Q(4)$	$101\,439.960 \pm 0.001$	0.000
$P(2)$	$101\,442.474 \pm 0.001$	0.001
$P(3)$	$101\,436.168 \pm 0.001$	0.000
$P(4)$	$101\,428.700 \pm 0.001$	0.001
$P(5)$	$101\,420.066 \pm 0.001$	-0.001

$\text{cm}^{-1}$ .<sup>14</sup> The absolute frequency position of the  $N_2$  lines is related, via the etalon markers, to this reference line. From a series of measurements a value for the transition frequency is obtained with a ( $2\sigma$ ) accuracy of  $0.001\text{ cm}^{-1}$  or  $30\text{ MHz}$ . As outlined previously<sup>13,15</sup> some systematic effects should be accounted for in evaluating absolute transition frequencies. Similar to previous work the residual Doppler shift was addressed by varying the flow speed of the nitrogen molecules in the molecular beam expansion. The effect of a net shift of the resonance frequency by frequency chirp generated in the dye amplifier<sup>15</sup> was not addressed in the present study. Since the measured  $N_2$  resonances are in a small wavelength interval it is a valid assumption that the frequency separations between lines are not affected by this chirp; in the absolute frequencies, chirp may result in a maximum uncertainty of  $100\text{ MHz}$  or  $0.0033\text{ cm}^{-1}$ . In Table I the measured frequency positions of  $N_2$  resonances are listed (neglecting this chirp-induced uncertainty), while in Table II the measured frequency separations are given. The absolute frequencies could in some cases be directly related to the “ $t$ ” components of lines in the  $B-X(v',1)$  bands of molecular iodine for  $v'=13-18$ , as presented in the work of Velchev *et al.*<sup>14</sup> However some  $N_2$  resonances were calibrated with respect to other  $I_2$  lines. These other reference lines, listed in Table III, were for the purpose of this study calibrated in our laboratory, following the procedures of Ref. 14.

The present absolute frequency positions and frequency separations between lines of the  $b^1\Pi_u-X^1\Sigma_g^+(1,0)$  band are included in a combined least-squares fit with the lower resolution data of Ref. 10 using the following energy expression:

TABLE II. Frequency separations between sets of lines in the  $b^1\Pi_u-X^1\Sigma_g^+(1,0)$  band of  $N_2$ .

Lines	Frequency separation (MHz)	Obs.-calc.
$R(1)-R(3)$	$5\,663 \pm 27$	-25.5
$R(0)-R(4)$	$11\,374 \pm 25$	-39.5
$R(1) \pm R(2)$	$14\,578 \pm 50$	64.6
$Q(1)-R(5)$	$17\,687 \pm 50$	23.0

TABLE III. Frequencies of newly calibrated reference lines of  $I_2$ . In all cases we refer to the “ $t$ ” hyperfine component (Ref. 14).

Assignment	Frequency ( $\text{cm}^{-1}$ )
$B-X(15,2)P85$	$16\,908.111\,61 \pm 0.000\,07$
$B-X(15,2)R91$	$16\,905.914\,06 \pm 0.000\,07$
$B-X(16,2)P126$	$16\,907.567\,13 \pm 0.000\,07$
$B-X(16,2)P127$	$16\,904.700\,45 \pm 0.000\,07$
$B-X(16,2)R131$	$16\,906.588\,66 \pm 0.000\,07$

$$E(J) = \nu_{10} + B[J(J+1) - 1] - D[J(J+1) - 1]^2 + q[J(J+1) - 1], \quad (1)$$

where the last term proportional to the  $\Lambda$ -doubling parameter  $q$  only holds for the levels of ( $f$ ) symmetry probed in the  $Q$  branch. The data points were weighted in the fit according to their uncertainties to derive a weighted  $\chi^2$  value. The present absolute frequencies are included with the uncertainty of  $0.001\text{ cm}^{-1}$ , while the frequency separations were given the uncertainties as listed in Table II. For the older data from Ref. 10 uncertainties of  $0.03\text{ cm}^{-1}$  (for the lower  $J$ ) and  $0.06\text{ cm}^{-1}$  (for  $J > 18$ ) were taken; blended lines were given an uncertainty of  $0.15\text{ cm}^{-1}$ . We found that the  $R(2)$  line in Ref. 10 contained a typing error and should read  $101\,456.602\text{ cm}^{-1}$ . For the electronic ground state, improved parameters have become available in recent years. We adopt the constants derived from a simultaneous reanalysis of several bands by Trickl, Proch, and Kompa;<sup>16</sup>  $B_0 = 1.989\,577\,6(1)\text{ cm}^{-1}$ ,  $D_0 = 5.741\,37(100) \times 10^{-6}\text{ cm}^{-1}$ ,  $H_0 = 4.843(1.000) \times 10^{-12}\text{ cm}^{-1}$ . These ground state constants were kept fixed in the fit.

The weighted fit resulted in a summed  $\chi^2$  of 104 for the set of 84 data points. This implies that the uncertainties are somewhat underestimated. However this underestimation is not in the presently obtained highly accurate data; for the 12 data points a summed  $\chi^2$  of 7 is obtained. Because of this internal consistency these data were not assigned with an uncertainty related to the possible overall shift of  $0.003\text{ cm}^{-1}$  due to the frequency chirp in the laser. The resulting molecular constants for the  $b^1\Pi_u$ ,  $v=1$  excited state are presented in Table IV. The stated uncertainties represent  $1\sigma$ . The rotational constants  $B$  and  $D$  are in agreement with previous findings within  $2\sigma$ . The  $\Lambda$ -doubling parameter  $q$ , previously not included, does not significantly differ from zero even with the high precision measurements. The band origin  $\nu_0$  is lower by  $0.05\text{ cm}^{-1}$  with respect to the previous lower resolution study.<sup>10</sup> This systematic shift is reflected in the data sets of the present and previous experiments; the presently

TABLE IV. Molecular constants for the  $b^1\Pi_u$ ,  $v=1$  state of  $N_2$  derived from absolute line positions (Table I), frequency separations (Table II), and values from Ref. 10. All values in  $\text{cm}^{-1}$ .

$\nu_0$	$101\,453.0022 \pm 0.0006^a$
$B$	$1.408\,05 \pm 0.000\,06$
$D$	$1.589 \times 10^{-5} \pm 7 \times 10^{-8}$
$q$	$-4 \times 10^{-5} \pm 4 \times 10^{-5}$

<sup>a</sup>This value follows from the least-squares fit; due to the chirp effect a possible systematic error of  $0.003\text{ cm}^{-1}$  should be taken as the true value.

obtained frequencies are on average lower by  $0.05\text{ cm}^{-1}$ . We have no explanation for this discrepancy. In view of the much higher resolution in the present study and the improved absolute calibration method the present data are more reliable. This implies that the values of Ref. 10 might have to be shifted by  $0.05\text{ cm}^{-1}$ .

## B. Linewidth measurements

Linewidth measurements were performed in two different campaigns separated by half a year. In the first campaign the focus was on the line broadening in the  $b^1\Pi_u$ ,  $v=1$  state. The geometrical configuration of the pulsed valve delivering the  $N_2$  beam and the skimmer were identical to the one used in the previous study on the  $c'_4\,^1\Sigma_u^+$ ,  $v=0$  state.<sup>5</sup> A difference with respect to that study is that the slit diaphragm, previously inserted in the time of flight to select ions from the central part of the interaction region (see Fig. 1 of Ref. 5) is now removed. This gives rise to a somewhat larger instrument width; from measurements of a krypton resonance ( $5p^6-6s'$  at  $95.34\text{ nm}$ ) it is estimated to be  $350 \pm 50\text{ MHz}$ . The line broadening of single, rotationally resolved lines in the  $b^1\Pi_u-X\,^1\Sigma_g^+(1,0)$  band was determined for all 100 recordings used in the spectroscopic analysis; since no dependence on rotational quantum number is observed an average was determined for all  $J$  levels. The resulting value is:  $\Delta\nu_{\text{obs}} = 475 \pm 10\text{ MHz}$  for fits of the observed line shapes to a Voigt profile, where the error corresponds to a  $1\sigma$  statistical uncertainty. In view of the rather large uncertainty in the instrument width, the uncertainty in its profile and the small difference between observed width and instrument width we can only give here a crude estimate of the lifetime for the  $b^1\Pi_u$ ,  $v=1$  state, based on considerations similar to those of Ref. 5. One of the procedures followed was a numerical deconvolution of the instrument profile obtained by recording the krypton resonance from the measured profile of the somewhat broader  $N_2$  resonance. Furthermore, deconvolution-based analytical procedures was used, one in which the instrument profile was taken as a Gaussian and one for a Lorentzian profile. A conservative estimate of the error was derived from a comparison between these methods. The estimate is  $\tau_{(v=1)} = 1.1\text{ ns} (+0.3; -0.2)$ .

Studies on effects of power broadening and radiation trapping were specifically focused on the  $c'_4-X(0,0)$  band, but some procedures were repeated for the  $b-X(1,0)$  band. Linewidth measurements were performed at various molecular densities in the beam and for a range of various intensities of the XUV and the fundamental UV. In general the conversion efficiency to the XUV is so low that the effect of population depletion by the ionizing UV is stronger than saturation by the XUV beam; the effect of depletion by the powerful UV beam was investigated in detail on the He atomic resonance.<sup>15</sup> Even for the  $c'_4-X(0,0)$  band, the one with the largest oscillator strength, no power broadening was observed. The same holds for radiation trapping; in case of the  $c'_4-X(0,0)$  band 90% of the population decays back to the  $X\,^1\Sigma_g^+$ ,  $v=0$  ground state. On the  $5p^6-6s'$  krypton resonance radiative trapping could be observed however, al-

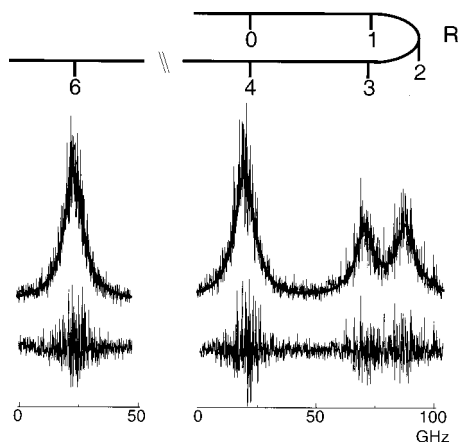


FIG. 2. Spectral recording of the bandhead region of the  $b^1\Pi_u-X^1\Sigma_g^+$  (4,0) band of  $N_2$  at  $\lambda=96.57$  nm. The width of the  $N_2$  lines is entirely determined by the short predissociation-induced natural lifetime. The lines were fitted to Lorentzian profiles; residuals are given below.

beit in a fluorescence decay experiment in our setup. For all excited  $b^1\Pi_u-X(v,0)$  bands the oscillator strength is less than for  $c'_4-X(0,0)$  and the relative decay toward  $X^1\Sigma_g^+$ ,  $v=0$  is much less than 90% because of the shift of the potential energy curve toward large internuclear separation. Moreover for  $b^1\Pi_u$ ,  $v>1$  states the predissociation channel is dominant. So in these cases, radiative trapping plays no role.

In a recent campaign, lifetimes of the  $b^1\Pi_u$ ,  $v=4, 5$ , and 6 levels were addressed. Several recorded spectra of resonance lines in excitation of these levels are displayed in Figs. 2–4. Linewidths derived from these and other spectra are listed in Table V; observed line shapes were in most cases fitted to Lorentzian profiles. During these measurements a skimmer with a slightly larger diameter was used in the experimental setup. The instrument width was determined from a remeasurement of the widths of the  $c'_4^1\Sigma_u^+$ ,  $v=0$  and the  $b'^1\Sigma_u^+$ ,  $v=1$  states, yielding now values of  $580\pm 50$  and  $500\pm 50$  MHz, respectively. As a result of the different geometry the observed widths are larger than in

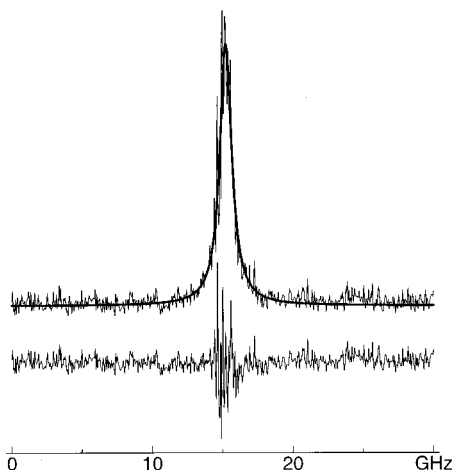


FIG. 3. Spectrum of the  $R(7)$  line in the  $b^1\Pi_u-X^1\Sigma_g^+$  (5,0) band of  $N_2$  at  $\lambda=95.52$  nm. The spectrum was fitted to a Lorentzian with  $\Delta\nu_L=1022$  MHz; residuals are also shown.

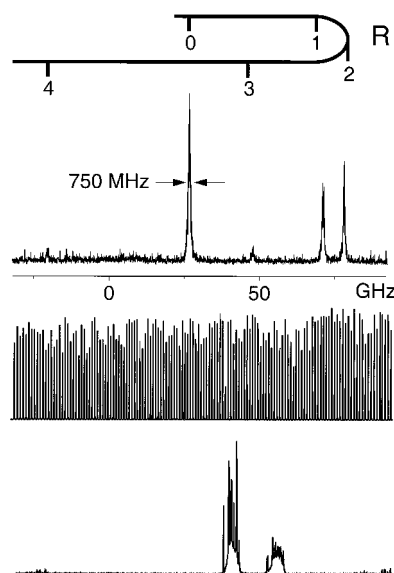


FIG. 4. Spectral recording of the bandhead region of the  $b^1\Pi_u-X^1\Sigma_g^+$  (6,0) band in a cold expansion of  $N_2$  at  $\lambda=94.92$  nm.  $I_2$  lines, P48(19-1) and R61(24-3), may be used for future absolute calibration.

previous measurements, when 515 and 460 MHz were obtained. Moreover in the same geometrical configuration an argon resonance line, however at a different wavelength of 105 nm,<sup>17</sup> was observed with a near-Lorentzian line shape of 450 MHz width. From this we conclude that the instrument width now is in the range 350–400 MHz. In Fig. 2 an example is shown of several lines near the bandhead of the (4, 0) band. The broad spectral profiles of 9 GHz full width at half-maximum fit nicely to a Lorentzian curve; the residuals from a fit only show an increase of noise near line center. The same holds for the much narrower  $R(7)$  line in the (5, 0) band shown in Fig. 3.

The broadening due to the natural lifetime can be obtained after deconvolving the instrument width from the values of the observed widths listed in Table V; however no analytical expressions exist in the case of composite line shapes involving Gaussian and Lorentzian contributions. This issue has been widely addressed in the literature and in the previous study<sup>5</sup> numerical analyses were used to find an approximate and simplified deconvolution procedure. There subtraction of a certain value (215 MHz) yielded reliable results when compared with numerical deconvolution tests. In view of the larger instrument width and its near Lorentz-

TABLE V. Observed linewidths  $\Delta\nu_{\text{ODS}}$  for some selected excited states of  $^1\Pi_u$  symmetry in  $N_2$ . The widths of the  $^1\Sigma_u^+$  states were used for calibration purposes.

Upper state	$\Delta\nu_{\text{ODS}}$ (MHz)	Line profile
$b^1\Pi_u$ , $v=1$	$475\pm 20$	Voigt <sup>a</sup>
$v=4$	$9200\pm 300$	Lorentzian
$v=5$	$1080\pm 80$	Lorentzian
$v=6$	$760\pm 80$	Lorentzian
$o_3^1\Pi_u$ , $v=0$	$960\pm 110$	Lorentzian
$b'^1\Sigma_u^+$ , $v=1$	$500\pm 50$	Voigt
$c'_4^1\Sigma_u^+$ , $v=0$	$580\pm 50$	Lorentzian

<sup>a</sup>Measured in a different geometry yielding smaller instrument width (see the text).



TABLE VI. Deduced lifetimes  $\tau$  for some selected excited states of  $^1\Pi_u$  symmetry in  $N_2$ .

Upper state	$\tau$ (ps)	Ref.
$b^1\Pi_u, v=0$	$16 \pm 3$	10
$v=1$	$1100 (+300; -200)$	This work
$v=2$	$10 \pm 2$	10
$v=3$	$1.6 \pm 0.3$	10
$v=4$	$18 \pm 1$	This work
$v=5$	$205 \pm 25$	This work
$v=6$	$350 \pm 75$	This work
$v=7$	$>150$	18
$v=8$	$>150$	18
$v=10$	$>150$	18
$v=11$	16	18
$v=12$	$>150$	18
$c_3^1\Pi_u, v=0$	$67 \pm 7$	5
$v=4(e)^a$	$76 \pm 20$	25
$o_3^1\Pi_u, v=0$	$240 \pm 50$	This work
$v=3$	$300 \pm 45$	11

<sup>a</sup>(e) Value pertains only to levels of (e) or  $\Pi^+$  symmetry.

ian profile in the present series of measurements we estimate that subtraction of 300 MHz from the observed widths (in the case of Lorentzian profiles) is appropriate. This estimate is certainly correct if we allow for an additional systematic uncertainty of 80 MHz due to deconvolution. Resulting values of the natural lifetime broadening  $\Gamma$  are then converted into a value for the lifetime via:  $\tau = 1/2\pi\Gamma$ . Values for  $\tau$  are listed in Table VI. Uncertainties in the derived values are calculated taking the combined statistical error in the measurement (see Table V) and the systematic error from the deconvolution procedure. In Table VI also other recently obtained values for lifetimes pertaining to  $^1\Pi_u$  states are listed.

#### IV. DISCUSSION AND CONCLUSION

Ultrahigh resolution XUV-excitation spectra of the  $b^1\Pi_u - X^1\Sigma_g^+(1,0)$  band have been recorded. Techniques of pulsed-dye amplification and harmonic generation, in combination with on-line saturation spectroscopy of  $I_2$  have been applied to determine absolute frequencies of  $N_2$  transitions in the XUV domain with unprecedented accuracy. These techniques could also be employed for other bands, but in the corresponding wavelength ranges no  $I_2$  frequency standards are available yet. Future calibrations could easily deliver absolute transition frequencies in the (5,0) and (6,0) bands with almost the same accuracy.

Line broadening in the  $b^1\Pi_u - X^1\Sigma_g^+$  band system was observed before;<sup>10,18</sup> however the resolution is now increased by a factor of 20. This improvement opens 100–500 ps dynamic ranges for lifetime studies by investigation of line broadening. While previously an upper limit of 150 ps was set for the lifetimes of the  $b^1\Pi_u$   $v=1, 5$  and 6 levels, now more accurate values are obtained. Some discrepancy is found in the measurements on  $b^1\Pi_u$   $v=4$ , where previously  $11 \pm 2$  ps was obtained.<sup>10</sup> For this 70% discrepancy we have no direct explanation. It should be considered, however, that in the previous study an instrumental width of  $0.27 \text{ cm}^{-1}$  had to be deconvoluted from an observed width of  $0.60 \pm 0.07 \text{ cm}^{-1}$ . In the present study the observed width of

9000 MHz is not at all affected by the instrument width of 300–400 MHz; moreover the present study gives a longer lifetime and a narrower line. Since experimental artifacts are bound to yield additional broadening, the present values can be considered as the reliable ones.

The resolution of the XUV laser source is barely sufficient to determine an accurate lifetime of  $b^1\Pi_u$   $v=1$ . The value of  $\tau = 1100(^{300}_{-200})$  ps is somewhat outside the limits of a previous value  $\tau = 1750 \pm 250$  ps.<sup>11</sup> The pump-probe laser-based method, recently used to determine lifetimes of CO, seems the appropriate method to derive improved lifetimes in the range near 1 ns.<sup>19</sup>

For aeronomic purposes it is important to produce values for the predissociation yields. To assess the competition between dissociative and radiative decay an estimate has to be made of the radiative lifetime of the excited states. Radiative decay rates  $A_{v'v''}$  are related to partial oscillator strengths  $f_{v'v''}$  via

$$f_{v'v''} = \left( 4\pi\epsilon_0 \frac{m_e c}{8\pi^2 e^2} \right) \lambda_{v'v''}^2 A_{v'v''}.$$

We assume that the  $\Lambda$ -doublet degeneracy of the excited state<sup>19,20</sup> is implicitly accounted for by the groups that performed the measurements on oscillator strengths.<sup>4,21,22</sup> The partial oscillator strength can be written as  $f_{v'v''} = fR_{v'v''}$  where  $R$  is a branching ratio. Now we focus first on  $b^1\Pi_u$   $v=1$ , for which the most extended data set is available. For the oscillator strength a value of  $f=0.156$  is reported<sup>4</sup> while the branching ratios for emission from this  $v'=1$  level into the  $v''$  manifold is measured; these values are listed in Table V of Ref. 4. Using this information and summing over all decay channels we obtain

$$A_{(v'=1)} = \sum_{v''} A_{(v'=1)v''} = 10.4 \times 10^8 \text{ s}^{-1},$$

corresponding to a radiative lifetime of 960 ps. The oscillator strength derived by James *et al.*<sup>4</sup> is smaller than other values in the literature:  $f=0.283$ <sup>21</sup> and  $f=0.243$ ;<sup>22</sup> these values would correspond to radiative lifetimes in the range 500–600 ps. In the work of Walter, Cosby, and Helm<sup>2</sup> a radiative decay of  $5.1 \times 10^8 \text{ s}^{-1}$  is deduced; this would correspond to a radiative lifetime of 1900 ps. In the following we adopt  $\tau_{\text{rad}} = 960$  ps and in view of the fact that radiation from all  $b^1\Pi_u$   $v$  levels is in the same wavelength window this value is assumed to hold for all  $v$ . The predissociation yield can be derived via

$$\eta_{\text{predis}} = 1 - \frac{\tau}{\tau_{\text{rad}}},$$

resulting in predissociation probabilities of 98% for  $v=4$ , 79% for  $v=5$ , and 63% for  $v=6$ .

These values markedly differ from those derived in studies of electron collision-induced emission from  $N_2$ ,<sup>4</sup> where for  $v=6$  a predissociation yield of 95.6% is deduced. For  $v=4$  and 5 James *et al.* obtain 100% predissociation. The latter result is also in contradiction with the finding of Roncin and Launay,<sup>12</sup> who measured in high resolution emission originating from the  $b^1\Pi_u$   $v=5$  level in eight different

bands. In other studies electron-induced emission was observed from the  $v=5$  level.<sup>23,24</sup> At present we have no explanation for the discrepancies in derived predissociation yields. For the  $b\ ^1\Pi_u\ v=1$  level the presently obtained lifetime is not very accurate; it would be consistent with a predissociation rate of 10% as reported in Ref. 4.

## ACKNOWLEDGMENT

This work was financially supported by the Netherlands Foundation for Fundamental Research of Matter (FOM).

- <sup>1</sup>R. R. Meier, *Space Sci. Rev.* **58**, 1 (1991).
- <sup>2</sup>C. W. Walter, P. C. Cosby, and H. Helm, *Phys. Rev. A* **50**, 2930 (1994).
- <sup>3</sup>H. M. Stevens, R. R. Meier, R. R. Conway, and D. F. Strobel, *J. Geophys. Res. B* **99**, 417 (1994).
- <sup>4</sup>G. K. James, J. M. Ajello, B. Franklin, and D. E. Shemansky, *J. Phys. B* **23**, 2055 (1990).
- <sup>5</sup>W. Ubachs, *Chem. Phys. Lett.* **268**, 201 (1997).
- <sup>6</sup>T. Birge and J. J. Hopfield, *Astrophys. J.* **68**, 257 (1928).
- <sup>7</sup>P. K. Carroll and C. P. Collins, *Can. J. Phys.* **47**, 563 (1969).
- <sup>8</sup>D. Stahel, M. Leoni, and K. Dressler, *J. Chem. Phys.* **79**, 2541 (1983).
- <sup>9</sup>M. Leoni and K. Dressler, *J. Appl. Math. Phys. (ZAMP)* **22**, 794 (1971).
- <sup>10</sup>W. Ubachs, L. Tashiro, and R. N. Zare, *Chem. Phys.* **130**, 1 (1989).
- <sup>11</sup>H. Oertel, M. Kratzat, J. Imschweiler, and T. Noll, *Chem. Phys. Lett.* **83**, 552 (1981).
- <sup>12</sup>J.-Y. Roncin and F. Launay, *Astron. Astrophys., Suppl. Ser.* **332**, 1173 (1998).
- <sup>13</sup>W. Ubachs, K. S. E. Eikema, W. Hogervorst, and P. C. Cacciani, *J. Opt. Soc. Am. B* **14**, 2469 (1997).
- <sup>14</sup>I. Velchev, R. van Dierendonck, W. Hogervorst, and W. Ubachs, *J. Mol. Spectrosc.* **187**, 21 (1998).
- <sup>15</sup>K. S. E. Eikema, W. Ubachs, W. Vassen, and W. Hogervorst, *Phys. Rev. A* **55**, 1866 (1997).
- <sup>16</sup>T. Trickt, D. Proch, and K. L. Kompa, *J. Mol. Spectrosc.* **171**, 374 (1995).
- <sup>17</sup>I. Velchev, W. Hogervorst, and W. Ubachs, *J. Phys. B* **32**, L511 (1999).
- <sup>18</sup>W. Ubachs, K. S. E. Elkema, and W. Hogervorst, *Appl. Phys. B: Photophys. Laser Chem.* **57**, 411 (1993).
- <sup>19</sup>P. Cacciani, W. Ubachs, P. C. Hinnen, C. Lyngå, A. L'Huillier and C.-G. Wahlström, *Astrophys. J. Lett.* **499**, L223 (1998).
- <sup>20</sup>D. C. Morton and L. Noreau, *Astrophys. J., Suppl. Ser.* **95**, 301 (1994).
- <sup>21</sup>E. C. Zipf and R. W. McLaughlin, *Planet. Space Sci.* **26**, 449 (1978).
- <sup>22</sup>W. F. Chan, G. Cooper, R. N. S. Sodhi, and C. E. Brion, *Chem. Phys.* **170**, 81 (1993).
- <sup>23</sup>H. D. Morgan and J. E. Mental, *J. Chem. Phys.* **78**, 1747 (1983).
- <sup>24</sup>E. C. Zipf, R. W. McLaughlin, and M. R. Gorman, *Planet. Space Sci.* **27**, 719 (1979).
- <sup>25</sup>H. Helm, I. Hazell, and N. Bjerre, *Phys. Rev. A* **48**, 2762 (1993).